Predicting the Effect of Alloy Composition on the Intermetallic Phase Transformation Kinetics in 6XXX Extrusion Alloys

N.C.W. Kuijpers[1], F.J. Vermolen[2], C. Vuik[2], S. van der Zwaag[3]

[1] Netherlands Institute for Metals Research, Delft, the Netherlands
[2] Department of Applied Mathematical Analysis, Delft University of Technology, Delft, the Netherlands
[3] Faculty of Aerospace Engineering, University of Technology, Delft, the Netherlands

Abstract

During the homogenisation treatment of 6XXX aluminum alloys a transformation of detrimental plate-like β-Al_5FeSi particles to desirable rounded α-$Al_{12}(FeMn)_3Si$ particles takes place. In this work the influence of the alloy composition, in particular the effect of Mg, Fe, Mn and Si, on the rate of this transformation is studied. A FEM model, linked to a thermodynamic database, is presented which can predict the influence of Mn and Si concentration on the β-to-α transformation rate. Interfacial Fe concentrations play a crucial role in the kinetics. The results of the model are in good agreement with experimental data.

1. Introduction

As cast aluminium extrusion billets can not be used for hot extrusion, primarily because their microstructure contains plate-like β-Al_5FeSi particles. In a so-called homogenisation treatment these β particles transform into smaller and rounded α-$Al_{12}(FeMn)_3Si$ particles. Once the transformation has taken place the material is suitable for producing high quality extrusion products. Understanding this phase transformation, ensuing particle shape change and its kinetics is a scientific challenge and of great industrial interest. Although the occurring processes are very complex and not yet fully understood, it would be highly desirable to have a validated approximate model for the transformation kinetics as a function of the many composition and metallurgical parameters. A recent general model for this transformation has been presented in [1,2]. In this paper the model is utilised to predict the effect of the alloy composition, in particular the effect of Mn and Si levels, on the kinetics of this transformation.

2. The Al-Fe-Si-Mn Phase Diagram

Figure 1a visualises the aluminium corner of the Al-Fe-Si phase diagram [3-5] which is a good approximation of the phase diagram of Mn free AA 6xxx alloys. As Mn-free AA 6xxx alloys contain small amounts of Fe and Si, the phase diagram indicates that only the

hexagonal α_h-Al$_8$FeSi or the β-AlFeSi phases are stable in the Al matrix. The other phases in Figure 1a, such as Al$_3$Fe, AlFeSi$_2$ and Al$_3$FeSi only occur for high Fe and Si levels. Note that in this Al-Fe-Si phase diagram the cubic α phase (α_c) is not present, since a minimum Mn content is required to stabilise it.

Figure 1b shows an enlargement of the calculated aluminium corner of the Al-Fe-Si phase diagram at a temperature of 540°C, The graph shows that the maximum solubility of Fe in Al is considerably lower (~0.015 wt.%) than the maximum solubility of Si (~1 wt.%). Figure 1b shows that high, intermediate, and low Fe/Si alloy-content-ratios lead to stabilisation of the Al$_3$Fe, α_h and β phases respectively. The effect of the Fe/Si ratio and the Si level on the stability of the phases has been confirmed experimentally [6,7].

The alloy composition of 6xxx alloys is designed such that the stable intermetallic phase is the α phase. For example, for a lowly Si alloyed AA 6xxx system (e.g. 0.6 wt.%) a low Fe alloy content (~0.20 wt.%) is required, whilst for a highly Si alloyed 6xxx system (e.g. 1.5 wt.%) a higher Fe content is required (~0.5 wt.%).
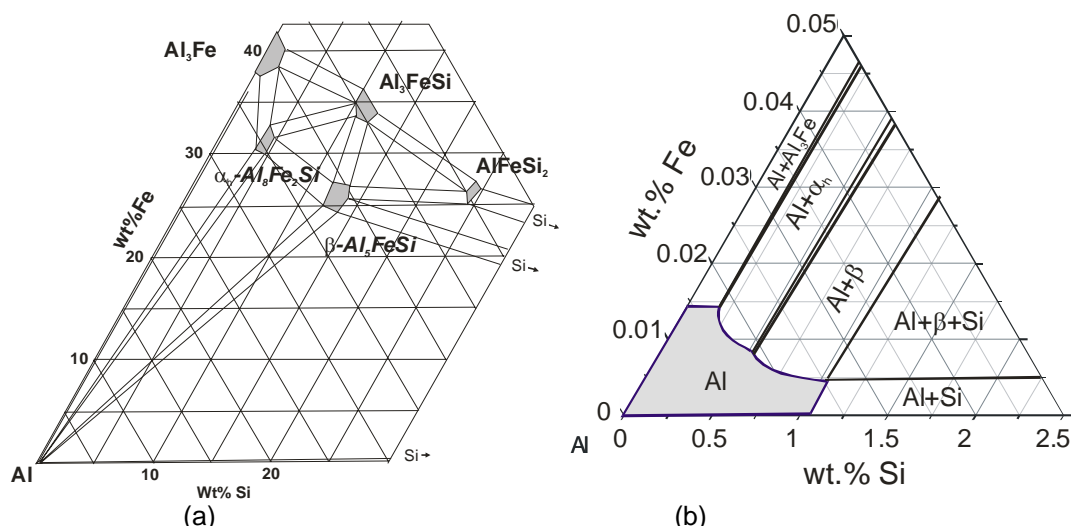

Figure 1: (a) The Al-corner of the Al-Fe-Si phase diagram [1]. (b) Enlargement of the Al-corner of the calculated Al-Fe-Si phase diagram, as derived by Thermo-Calc for a temperature of 540°C. Note that, in this graph, the Fe-scale is enlarged.

3. The Model

Figure 2 shows a schematic representation of the particle and matrix as modelled in the FE-Model. For the model cylindrical co-ordinates are used where the line AH is the axis of symmetry. This geometry presents a piece of the original β-plate with one α nucleus on top of it. The FE-Model describes the growth of the α-particle towards the dissolving rim S_β of the β-plate. During the transformation, the thickness of the β plate remains constant. The α particle grows along the entire α/Al interface, indicated by S_α. The transformation is assumed to be diffusion controlled, and its driving force is given by the difference in chemical potential. Fe and Si diffuse from the β rim through the aluminium matrix towards the α particle. Since the diffusion speed of Fe is a few orders lower than that of Si, only the diffusional fluxes of Fe are dealt with in the model as Fe diffusion is

rate limiting. The velocities of the moving boundaries S_α and S_β are derived by the use of the Stefan condition [8], considering the equilibrium interface concentration, and the diffusion flux at the boundary. All FEM calculations are performed using the software package SEPRAN, which has been developed at the Department of Applied Mathematics at the Delft University of Technology, The Netherlands.
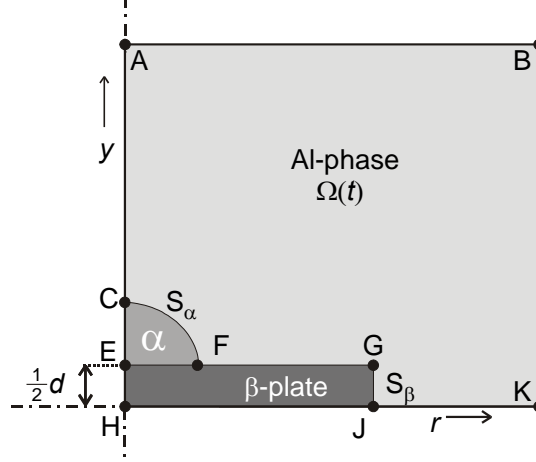

Figure 2: The geometry of the domain of computation of an α particle on a β plate in an Al-phase. The parameters are explained in the text.

Table 1:Basic physical parameters which are used for the FE model calculations.

Parameter	Symbol	Value
Diffusion pre-factor [9]	D_0	$5.3 \cdot 10^{-3}$ m^{2}s^{-1}
Activation energy of diffusion [9]	Q	183.4 kJ/mol
Fe concentration in α particle [10]	c_α^p	39.9 wt.%
Fe concentration in β particle [10]	c_β^p	33.9. wt.%
Initial radius of α particle	r_α^{init}	0.25 μm
Thickness of β-plate	D	0.2 μm
Equivalent Diameter of initial β-plate	l	1.5 μm
Cell size of aluminium matrix	l_{cell}	2.5 μm
Temperature	T	853 K (580°C)

Table 1 presents the global model parameters used for the FE calculations. The geometrical parameters, such as initial radius of the α particle, initial thickness, and initial diameter of the β plate were obtained experimentally. In the calculations, it is assumed that the geometrical starting parameters are not affected by the variation of the matrix content in Si and Mn level nor by temperature.

As demonstrated elsewhere [1,11] we argue that the main driving force of the transformation is the difference in chemical potential ($\Delta\mu_{Fe}$) of solute iron on the interfaces (S_α and S_β) of the phases in the aluminium alloy. This difference in chemical potential of the iron solute levels in the Al-phase close to the α (μ_α^s) and the β interface (μ_β^s), result in a diffusional flux of iron atoms towards the α phase. It is assumed that the interfacial reactions are fast enough to maintain local thermodynamic equilibrium concentrations at the α/Al and β/Al interface. The chemical potentials of Fe at the two interfaces depend on the solute levels of other elements, such as Si and Mn. Since the Finite Element Model is based on Fick's diffusion for the Fe-concentration in the Al-phase, we use the differences in the solute concentration between the α and β interfaces instead.

As an example we plot in Figure 3 the interfacial concentration levels at the matrix-α particle and the matrix-β particle at two temperatures, 540 and 580 ^{0}C, as a function of the Mn concentration. These concentration levels are key parameters in the model. In domain *I* representing Mn concentrations between 0 wt.% and 0.02 wt.%, the driving force Δc_{Fe} is negative or very small, and therefore the β-AlFeSi particles will not, or only slowly, transform by diffusion controlled transformation to the α-Al(FeMn)Si particles. In domain *II*, representing Mn alloy contents between 0.02 and 0.2, an addition of Mn increases the gradient and hence the expected speed considerably. In region *III*, with Mn concentration higher than 0.2 wt.%, the gradient remains high and does not significantly depend on the Mn content anymore. These qualitative predictions are in agreement with experimental data by Zajac *et al.* [6].
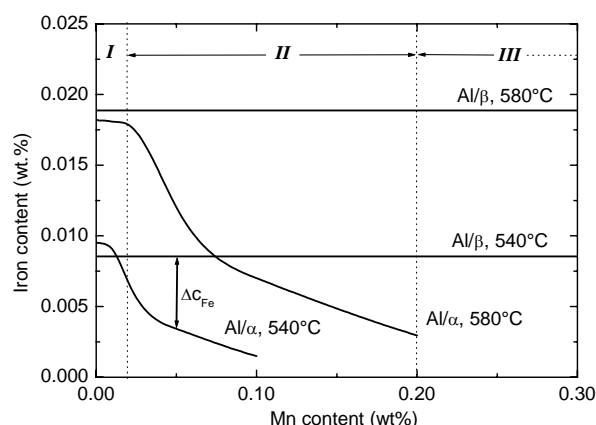

Figure 3: Plots of the interfacial matrix concentrations (c_{Fe}) as a function of the Mn matrix content. The results were obtained by Thermo-Calc. Plots are drawn for both Al/α and Al/β interfaces, at homogenisation temperatures of 540°C and 580°C. For the presented calculations a fixed matrix concentration of 0.5 wt.% Si is used.

4. Results

Using the interfacial concentrations as a function of the Mn and Si level in the matrix and the other fixed input parameters defined for the model we can now calculate quantitatively the increase in α volume with respect to the decreasing β fraction.

First, the influence of the Mn matrix content on the β-to-α transformation rate is investigated. For this example we took a fixed Si-matrix concentration of 0.3 wt.%. Figure 4 shows the transformed fraction as a function of time of various alloy Mn levels. Mn additions between 0 and 0.02 wt.% show a small effect on the transformation rate. However, Mn additions between 0.02 and 0.20 wt.% give a considerably larger effect on the transformation rate. It was found that Mn additions larger than 0.20 wt.% have almost no extra effect on the transformation rate anymore, since in this case the maximum Fe concentration difference between the α/Al and β/Al interface is achieved.

Figure 5 shows the transformed fraction as a function of time for various Si matrix concentrations. The figure shows that a variation of the Si concentration between 0.1 and 1 wt.% has a large influence on the transformation rate. Figure 5a shows the influence of Si in the case of a high Mn content of 0.2 wt.%. Figure 5b shows the influence of Si in the

case of a low Mn content of 0.02 wt.%. The figure indicates that, when decreasing the Mn content, the influence of Si on the transformation rate increases considerably. The cases of a Si matrix concentration of 0.6, 0.8 and 1.0 wt.% in Figure 5b are hypothetical, since in this case Δc_{Fe} is negative, and the finite element model derives a dissolution mechanism of the α particles, and the β particles will be stabilised.
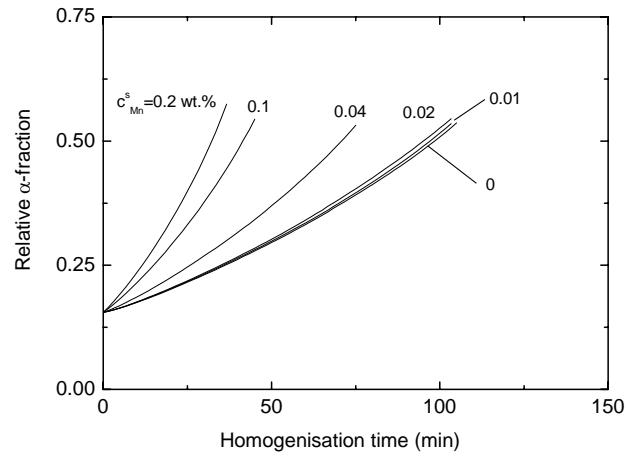

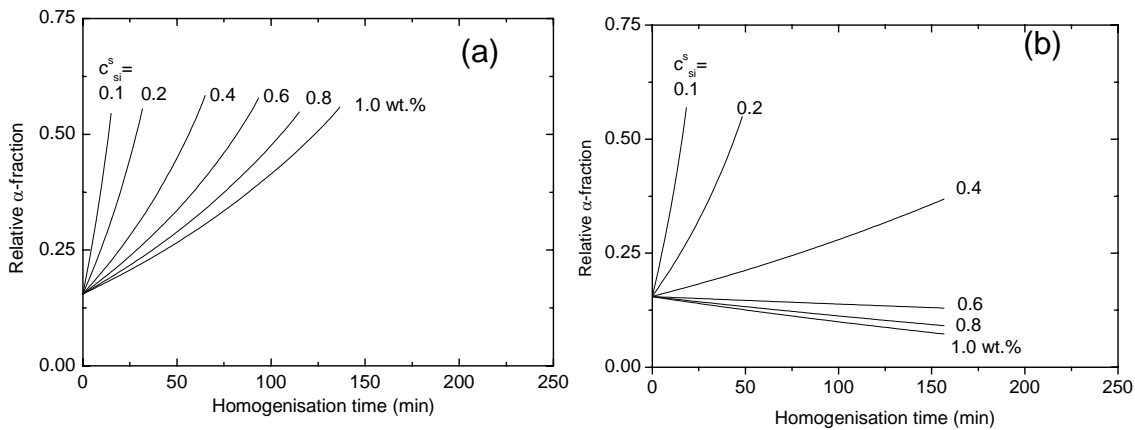Figure 4: Transformed fraction as a function of time at various Mn levels.

Figure 5: Transformed fraction as a function of time at various Si levels. (a) With a fixed Mn matrix concentration of 0.10 wt.%. (b) With a fixed Mn matrix concentration of 0.02 wt.%.

We investigate the combined effect of the Mn and Si matrix concentrations on the transformation time. Figure 6 shows the iso-time contours for various Mn and Si alloy contents. Each contour represents the Mn and Si content for which the transformation time up to a fraction of f_α=0.5 wt.% is the same.

The figure indicates that the transformation time could be short (30 minutes), for alloys with a low Si and a high Mn content. On the other hand, long homogenisation times, longer than 4 hours, are required for alloys with a high Si and low Mn content. In the extreme case, of a high Si content, and a Mn content lower than 0.02 wt.%, there is no transformation anymore. The dashed area in the diagram indicates the alloy compositions in which there is no transformation, i.e. conditions in which the β phase is the stable phase (see also Figure 5b).
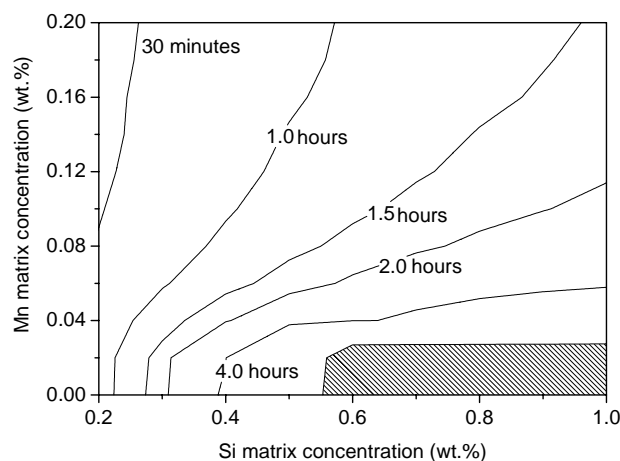
Figure 6: Iso-transformation-time contours for a window of Mn and Si compostions.

The predicted results presented above are in good agreement with industrial experience. The results of a large experimental program to validate the model are to be presented elsewhere [1,12] but it can already be stated that the model predicts the time for 50% transformation very well.

5. Conclusions

A Finite Element model in combination with a thermodynamic calculations of the Fe interfacial concentrations at the interfaces of both the α and β intermetallics was used to describe the influence of the alloy content on the β-to-α transformation rate. The model predicts a significant effect of the Si and Mn alloy content on the transformation kinetics. It was found that Mn has the largest effect on the transformation rate. Although not shown here, the model is well supported by experiments [12].

Acknowledgement

References

[1]	N.C.W. Kuijpers, PhD thesis, Delft University of Technology, 2004
[2]	N.C.W. Kuijpers, F.J.Vermolen, C.Vuik and S.van der Zwaag; Met. Mater Trans A 44, 1448-1456, 2003
[3]	V. Stefániay, A. Griger and T. Turmezey, J. Mat. Sci. 22, 539-546, 1987
[4]	A. L. Dons, Z. Metallkde 77, 126-130, 1986
[5]	A. L. Dons, Z. Metallkde 76, 609-612, 1985
[6]	S. Zajac, B. Hutchinson, A. Johansson and L. O. Gullman, Mat. Sci. Tech. 10, 323-333, 1994
[7]	Y. Langsrud, Key Engineering Materials 44-45, 95-116, 1990
[8]	G. Segal, C. Vuik and F. J. Vermolen, J. Comp. Phys. 141, 1-21, 1998
[9]	D. L. Beke, I. Gödény, I. A. Szabó, G. Erdélyi and F. J. Kedves, Philos. Mag. A5, 425-443, 1987.
[10]	L. F. Mondolfo: *Structure and Properties of Aluminium Alloys*. (Butter-worth, England, 1976).
[11]	F.J.Vermolen, N.C.W. Kuijpers, C.Vuik, P.T.G. Koenis, K.E. Nilsen and S. van der Zwaag. Proceeding Int. Conf. on Extrusion Technology 2004, Orlando, USA
[12]	N.C.W. Kuijpers, F.J. Vermolen, C. Vuik, S. van der Zwaag, to be published.